Accepted Manuscript

Surface Properties and fibre-matrix adhesion of man-made cellulose epoxy composites – influence on impact properties

A. Mader, A. Kondor, T. Schmid, R. Einsiedel, J. Müssig

PII: S0266-3538(15)30160-3

DOI: 10.1016/j.compscitech.2015.12.007

Reference: CSTE 6273

To appear in: *Composites Science and Technology*

Received Date: 10 June 2015

Revised Date: 9 December 2015

Accepted Date: 14 December 2015

Please cite this article as: Mader A, Kondor A, Schmid T, Einsiedel R, Müssig J, Surface Properties and fibre-matrix adhesion of man-made cellulose epoxy composites – influence on impact properties, *Composites Science and Technology* (2016), doi: 10.1016/j.compscitech.2015.12.007.

Surface Properties and fibre-matrix adhesion of man-made cellulose epoxy composites – influence on impact properties

Mader, A.[1,4], Kondor, A.[2], Schmid, T.[2], Einsiedel, R.[3] & Müssig, J.[1*]

[1] Hochschule Bremen – HSB - City University of Applied Sciences, Faculty 5, Biomimetics – The Biological Materials Group, Neustadtswall 30, 28199 Bremen, Germany

[2] Surface Measurement Systems (SMS), London, UK

[3] Cordenka GmbH GmbH & Co. KG, Industrie Center Obernburg, 63784 Obernburg, Germany

[4] now affiliated with the Institute of Building Structures and Structural Design (ITKE), University of Stuttgart, Germany

*corresponding author:

Prof. Dr.-Ing. Jörg Müssig

Hochschule Bremen - University of Applied Sciences

Faculty 5, Department Biomimetics – Biological Materials

Neustadtswall 30

D-28199 Bremen / Germany

Telephone: ++49 (0)421 5905 2747

Fax: ++49 (0)421 5905 2537

joerg.muessig@hs-bremen.de

1 Abstract

Previously conducted studies showed that UD regenerated cellulose reinforced thermoset composites can obtain specific Charpy impact strength values in the range of glass fibre reinforced composites. Composites of two different viscose fibre types, each with and without an oily avivage, were investigated. Despite similar mechanical properties of the fibres the impact strength of the *CR* fibre composites was about twice as high as the of the *standard* fibre composites.

To reveal a possible explanation for this effect the fibre surface properties were investigated more closely. AFM measurements showed no differences in fibre surface topologies. However the physico-chemical properties of the fibre types differ. IGC measurements showed that the *standard* Cordenka fibre without avivage (“*std wo a.”*) possesses a slightly higher specific surface energy and base number (K_b) than the *CR* fibres without avivage (“*CR wo a.”*) resulting in a better adhesion to the highly polar epoxy. This is also shown by the pair specific interaction parameters (I_{sp}), which is clearly higher for the neat epoxy – *“std wo a.”* pair, and by the higher work of adhesion between the neat epoxy and the *“std wo a.”* fibres. Accordingly the measured fibre pull-out lengths of the *CR* fibres are one order of magnitude higher than of the *std* which suggests a weaker interfacial shear strength between the *CR* fibres and epoxy. Within the same fibre type the samples without avivage show longer pull-out lengths. As a weaker fibre-matrix adhesion causes stronger crack deflection and energy dissipation these results correspond well with the previously measured Charpy impact strengths.

Keywords: A. Polymer-matrix composites (PMCs); B. Fibre/matrix bond; B. Impact behaviour; D. Atomic force microscopy (AFM); Inverse gas chromatography (iGC)

2 Introduction

Due to the growing environmental awareness the research in bio-based fibres and polymers for composites has grown remarkably in recent times. Besides the use of natural fibres regenerated cellulose fibres are an interesting alternative. Cellulose is dissolved and formed into endless fibres [1]. During this process important advantages of natural fibres such as the bio-based character and the low density are maintained [2] while some disadvantages of natural fibre like variability in quality or the limited length of the fibres are overcome. Usually bast fibres are used as reinforcing materials in composites as they exhibit a high stiffness and strength. However they are brittle in nature resulting in a low impact strength [3]. Regenerated cellulose fibres combine remarkable stiffness values and high elongations at break and thus can be used to produce fibre-reinforced composites that possess interesting impact and energy absorption properties. A previously published study [4] showed that UD regenerated cellulose fibre-reinforced thermoset composites can obtain specific Charpy impact strength values in the range of glass fibre composites with the same fibre content by mass. Two different viscose fibre types with identical Young's modulus and slightly different tensile strengths were compared and big differences in Charpy impact strengths were measured. The impact strength of samples with the fibre type developed especially for composite applications (*CR*) is twice as high as the values of samples with the common (*standard*) viscose fibres. This gap cannot be explained solely by the higher tensile strength of the *CR* fibres and the analysis of SEM images of fracture surfaces leads to the assumption that the adhesions of the fibres to the matrix differ.

It is well known that besides the properties of the constituents the interfacial shear strength between fibre and matrix plays an important role in the mechanical properties of composites. It provides the structural integrity of composites and determines the ability of the interphase to transfer load from the matrix to the embedded fibres. A higher interfacial shear strength

usually leads to a higher tensile and flexural strength [5–8] . However in the case of impact strength not only the modulus and strength but also the pull-out of fibres is an important property to control the fracture energy of a composite. During impact the important mechanisms of energy absorption are the debonding, the pull-out and the fracture of fibres. So in the case of impact strength a poor fibre-matrix adhesion can lead to an improvement of the properties. In a composite where the elongation at break of the fibres is greater than the one of the matrix a crack originates in the matrix and propagates in it until it reaches a fibre. With increasing load the crack extends around the fibre and along the fibre-matrix interface causing fibre debonding and crack extension. Eventually the fibre breaks at a random weak spot some distance away from the crack. During further composite failure the loose end of the fibre is pulled out of the matrix and energy is dissipated due to frictional forces. A high shear strength between fibre and matrix inhibits fibre crack deflection and thus reduces the fibre pull-out. Therefore a weaker fibre-matrix adhesion can cause higher impact strength values [9,10]. However it has to be kept in mind that a minimum of fibre-matrix adhesion is required in order to allow the transfer of stresses from the matrix to the fibre and ensure the reinforcing effect of the fibres.

The fibre-matrix adhesion is devided into a physico-chemical and a frictional component. The later one is due to mechanical interlocking at the interface. The physico-chemical adhesion between fibre and matrix is based on molecular interactions, as e.g. covalent and hydrogen bonds, intermolecular forces or transcristallinity [7,8,11]. In the case of composites with a polymer matrix the physico-chemical contribution is important and it is governed by the surface properties of the fibre and the matrix [7]. Important characteristics are the surface energies, the acid-base interactions and the thermodynamic work of adhesion. To better understand and tailor the adhesion between fibres and matrix the physico-chemical properties of various fibres and polymers were investigated with regard to their contribution to the fibre-matrix adhesion. Several reviews focus on the surface properties of natural or cellulose fibres

in combination with polymeric matrices [5,7,11,12]. Due to the hydrophilic character of natural or cellulose fibres, which is given by the hydroxyl groups of the cellulose, their bond to commonly used non-polar, hydrophobic matrices is low. Therefore different surface modification of cellulose fibres in order to reduce the hydrophilic character were the focus of several studies [5,11–14].

From the surface energetics of the fibre and the matrix the thermodynamic work of adhesion and the pair specific interaction parameter (I_{sp}) can be calculated. The surface energy of the fibres is directly related to the thermodynamic work of adhesion, which is directly correlateed to practical adhesion. A possiblity to enhance the fibre- matrix-adhesion is therefore to increase the surface energy of the fibre [11]. Also the acid-base interaction are an impotant factor as, if the fibre and the matrix would both be acidic or neutral only van der Waals forces would bond the fibre to the matrix [5]. An increase in acid-base interaction results in an higer interfacial shear stength [7]. Various authors found a correlation between the work of adhesion or the pair specific interaction parameters (I_{sp}) and the interfacial shear strength of composites [15,16] or investigated the contribution of the I_{sp} to the tensile properties of composites [5]. Tze et al. [7], Schultz et al. [15] and Mukhopadhyay et al. [17] found a linear correlation between the I_{sp} and some mechanical properties of the composites like interfacial shear resistance (τ).

To examine to surface properties of the fibres and the matrix, in order to investigate the adhesion potential of diffent fibres to a matrix, inverse Gaschromatography (iGC) can be used. IGC has been used before to characterize the surfaces of various different fibres [11,18]. Especially in the development of cellulose-polymer compoites iGC has been used to analyse the interface in composites. The method of iGC is better suited for the study of cellulosic fibre surfaces than wetting or contact angle measurements, where the surface roughness, the herterogenety of the probe or bulk pnenetration can cause a contact angle hysteresis [5].

IGC is a gas phase technique, first developed in the 1950s, to study surface and bulk properties of particulate and fibrous materials [19]. Apart from its high versatility and speed, the main benefit of iGC is its sensitivity at the surface of the sample. The iGC is the reverse of the analytical gas chromatography. The adsorbent under investigation is placed into a column while a known adsorptive is used in the gas phase. As in analytical gas chromatography, the retention time is obtained as the fundamental parameter measured. The retention time can be converted into a retention volume, which is directly related to several physico-chemical properties of the solid (absorbent). These properties can be thermodynamic parameters, such as surface energy or heat of sorption and kinetic parameters, such as the diffusion constant or the activation energy of diffusion. It is also possible to determine the uptake for both physisorption and chemisorption processes. In the first case, a sorption isotherm is obtained, which allows the computation of the surface area and heterogeneity profiles [20].

According to Riddle & Fowkes [21] the total surface energy of a material is often divided into two components: dispersive (London dispersion, van der Waals, Liftschitz interactions) and specific (acid-base, polar interactions).

$$\gamma_s^T = \gamma_s^{ab} + \gamma_s^d \qquad (1)$$

The dispersive surface energy (γ_S^D) analysis is performed by measuring the net retention volume V_N (measured retention volume corrected with dead volume) for a series of alkane elutants. The dead-volume is determined by an unretained solute. The dispersive surface energy can be determined with the Dorris and Gray method [22], plotting by the $RT\ln(V_N)$ versus the carbon number (of the alkanes) which produces a linear correlation. The dispersive component of the solid sample can be determined from the slope of the line

$$Slope = 2(\gamma_{CH_2}\gamma_S^D)^{1/2} * N_A a_{CH_2} \qquad (2)$$

where γ_S^D is the dispersive component of the solid surface energy, a_{CH_2} is the cross sectional area of a methylene group and N_A is Avogadro's number.

The specific contribution of the total surface energy is obtained via iGC SEA by first measuring the specific free energies of adsorption for different polar probe molecules (ΔG_{SP}). These values are determined by measuring the retention volume of polar probe molecules on the samples. In the polarisation approach [18], the ΔG_{SP} values are determined from a plot of $RT\ln(V_N)$ versus the molar deformation polarisation of the probes (P_D).

$$P_D = \{MW*(r^2-1)\}/\{D*(r^2+2)\}, \quad (3)$$

where MW is the molar mass of the probe, r is the reflective index of the probe and D is the probe liquid density. On the $RT\ln(V_N)$ versus P_D plot the points representing a polar probe are located above the alkane straight line and the vertical distance between the polar data point and the straight line is equal to the specific component of the free energy of adsorption of the polar probe [23]. From the ΔG_{SP} values of two monopolar probes, the specific surface energy (γ_S^{AB}) can be calculated by the van Oss approach [24]. The specific contribution is subdivided into an acid γ^+ and a base γ^- parameter of the surface tension of the mono-functional polar probes. In this approach, the Della Volpe scale is employed, with a pair of mono-functional acidic and basic probe molecules (dichloromethane (CH_2Cl_2) - γ^+ : 124.58 mJ/m^2 and ethyl ethanoate (ethyl acetate) ($C_4H_8O_2$) - γ^- : 475.67 mJ/m^2).

The approach of Gutmann represents the electron-accepting and electron-donating characteristics of the surface by the acid and base numbers (K_a and K_b) respectively. The K_a and K_b constants of a polymer (matrix of the composite) and fibre, may define the pair specific interaction parameters (I_{sp}) by the following expression [15,18],

$$I_{sp} = K_a^f K_b^m + K_a^m K_b^f \quad (4)$$

Where f and m corresponds to the fibre and the matrix, respectively.

The surface energy is directly related with the thermodynamic work of cohesion and adhesion and it can be calculated with the following expressions [6],

$$W_{Coh}^{Total} = 2\left[\left(\gamma_s^d\right) + \left(\gamma_s^- \cdot \gamma_s^+\right)^{1/2} + \left(\gamma_s^+ \cdot \gamma_s^-\right)^{1/2}\right], \quad (5)$$

$$W_{Adh}^{Total} = 2\left[\left(\gamma_{s1}^d \cdot \gamma_{s2}^d\right)^{1/2} + \left(\gamma_{s1}^- \cdot \gamma_{s2}^+\right)^{1/2} + \left(\gamma_{s1}^+ \cdot \gamma_{s2}^-\right)^{1/2}\right], \quad (6)$$

where γ_s^d is the dispersive surface energy component of the solid material, γ_s^- and γ_s^+ are the acid and base components of the specific surface energy of solid material, and the number 1 and 2 denote e.g. polymer and fibre, respectively.

Within this study the previously tested [4] viscose fibres are investigated more deeply in regard to their surface property and the interfacial shear strength. The differences in adhesion to the epoxy matrix are quantified by measuring the fibre-pull-out length with a separate experimental set up. Moreover the surface energy properties of the fibres are examined by inverse gas chromatography (iGC) to identify the reason for the differences in fibre-matrix adhesion.

3 Experimental

3.1 Materials

Within this work four samples of man-made cellulose fibres were examined. The common high quality viscose rayon Cordenka RT 610, in the following referred to as *standard (std)* fibre, and the *CR* rayon, especially developed for composite applications (Cordenka GmbH & Co. KG, Obernburg, DE). Both fibre types were provided with and without an oily avivage, labelled *"w a."* and *"wo a."* respectively. The avivage is a mixture of sulphated natural and synthetic oils. As matrix the epoxy resin RIM 135 and the hardener RIMH 137i (both supplied by Lange+Ritter GmbH, Gerlingen, DE, mixed with a ratio of 100:30 parts by weight) were used.

3.2 AFM

To examine the surface topology of the four fibre samples for possible differences an atomic force microscope (AFM) was used. The AFM measurements were carried out with a NanoWizard® AFM of JPK (Berlin, DE). For investigation the fibres were placed on an object slide with a double-faced adhesive tape (Tesa SE, Hamburg, DE). The measurements were done in contact mode with a scanning speed of 1 Hz and the scanning area was 5 x 5 µm². The used cantilever of the type Arrow, supplied from NanoWorld (Neuchâtel, Switzerland) had a spring rate of 0.2 N/m and a resonance frequency of 14 Hz.

3.3 IGC

To analyze the physico-chemical properties of the fibres the surface energy and the acid/base properties of the *std* fibre, the *CR* fibre and the cured neat epoxy were determined. As in this investigation the focus was on the differences between the *std* and *CR* fibres not all four fibre samples were investigated but only these without avivage to avoid possible influences of the avivage on the results. The epoxy was measured in the cured state, aware of the fact that the surface energy components of the uncured and cured epoxy might differ. In fact Abbot & Higgins [25] determined -0.074 mJ/m² experimental temperature coefficient of surface tension for the DGEBA/DGE epoxy. Similar values were found for polymer melds by Wu [26]. However only solid probes can be examined by the method iGC. As the interaction with *std* and *CR* fibres would be affected in the same way the comparison between the samples, what is the focus of this study, should still be valid.

The surface energy measurement was carried out with an inverse Gas Chromatography – Surface Energy Analyser (iGC-SEA) system which is the 2nd generation sorption instrument by Surface Measurement Systems Ltd., London, UK. The carrier gas was Helium (He) and methane (CH_4) was used to determine the dead time of the system. The controlling of the experiment and the data analysing were performed with the SEA Control and Analysis

Software. The relative standard deviation of the iGC-SEA system for the surface energy analysing using PEAK COM retention time is between 0.37 and 0.69 %. Due to this high reproducibility of the instrument the standard deviations are not shown in the graphs.

The surface energy and the acid/base properties of the individual components were determined at 30 °C and 0 % relative humidity (RH). The carrier gas was helium (He) and the applied solvents were octane (C_8H_{18}), nonane (C_9H_{20}), decane ($C_{10}H_{22}$) and undecane ($C_{11}H_{24}$), ethanol (C_2H_5OH), ethyl ethanoate (ethyl acetate) ($C_4H_8O_2$), dichloromethane (CH_2Cl_2), propan-2-one (acetone) (C_3H_6O) and acetonitrile (C_2H_3N).

Prior to any surface energy related experiments, the specific surface area of the sample was first determined by measuring the octane (C_8H_{18}) adsorption isotherms at 30 °C and 0 % RH using the iGC SEA. The BET specific surface area of the sample was subsequently calculated from the corresponding octane isotherm, within the partial pressure range of 5 % to 35 % P/P0.

3.4 Fibre pull-out length

The differences in interfacial shear strength were further quantified by measuring the fibre pull-out length of all four different fibre samples.

In composites stress is transferred from the matrix to the fibre, whereat the fibre-matrix adhesion is an important factor. The minimum fibre length necessary to transfer enough stress from the matrix to the fibre to reach its ultimate strength and cause fibre breakage is defined as the critical fibre length l_c. It depends on fibre diameter d, the ultimate fibre strength σ_F and the interfacial shear strength τ [27].

$$l_c = \frac{\sigma_F \cdot d}{2 \cdot \tau}$$

A higher interfacial shear strength leads to a reduced critical fibre length and thus fibre pull-out length. So measuring the fibre pull-out lengths is a method to characterize the interfacial shear strengths τ between fibre and matrix. The measurement of the fibre pull-out length was conducted according to Graupner et al. [28]. However the procedure was adapted for the use of a thermoset resin.

Due to the strong scattering of the collected data a large quantity of fibre pull-out lengths has to be measured. To obtain sufficient data 100 to 150 fibres were prepared as follows: Approximately ten single Cordenka fibres were placed unidirectionally on a glass slide covered with a Teflon foil. To achieve a parallel alignment and pretension of the fibres each fibre was first fixed on one side of the glass slide with an adhesive tape. To the other end of the fibre a pretensioning mass of 100 mg was applied. The fibre was brought into a position parallel to the neighbouring fibres and fixed there with an adhesive tape. As all fibres were prepared the mixed epoxy was put on the fibre with a fine brush until the fibres were covered completely. The resin was cured for 48 hours at room temperature. The resulting test specimens had a width of about 23 mm and a thickness of 0.2 - 0.5 mm. To ensure that the specimens break in the middle they were waisted from both sides with a radius of 200 mm. The width of the waisted specimens was approximately 23.5 mm.

The specimens were loaded axially in tension until failure with a Zwick/Roell universal testing machine Z020 (Zwick/Roell GmbH, Ulm, DE). A 500 N load cell and manually closable metal clamps (Typ 8133, 1 kN, Zwick/Roell GmbH) were used. The clamping length was 10 mm and the testing speed was 2 mm/min.

With a polarization microscope (Bresser Science ADL-601P, Bresser GmbH, Rhede, DE with Bresser Microcam 9.0 MP) a picture of each pulled-out fibre was taken and the fibre pull-out length was measured using ImageJ (U.S. National Institutes of Health, Bethesda, Maryland, USA).

If the fibre diameter and tensile strength are the same for all fibre types to be compared the measured pull-out lengths can be compared directly, as these two properties are besides the shear strength the only two factors influencing the pull-out length.

In case of differing fibre tensile strengths, as is here the case, a factor can be used to adjust the measured pull-out lengths. A lower tensile strength for example causes shorter pull-out lengths. As this relation is proportional a suitable factor can be calculated by normalizing the tensile strength of the fibres and dividing the measured pull-out lengths by it. So the corrected pull-out length is obtained which displays what the measured fibre-pull-out lengths would be if all fibre types had the same tensile strength.

4 Results and discussion

4.1 AFM

In Figure 1 the results of the AFM measurements are compared. There is no difference recognizable in the surface topology of the different samples. This suggests that the differences in the interfacial shear strengths are probably not only due to differing frictional forces caused by the fibre surface structure in the micro scale but are rather a result of the physico-chemical surface properties.

However to further verify this assumption the RMS roughness of the two fibre surfaces would have to be determined. But as Tze et al. stated while the frictional forces of the fibre-matrix adhesion dominate in ceramic composites, in physico-chemical interactions are consideravly important in composites with a polymer matrix [7].

4.2 IGC

The BET specific surface area values of the tested samples are listed in Table 1. Dispersive (γ_S^D), acid-base (γ_S^{AB}) and total surface energy (γ_S^T) profiles are obtained directly from the iGC SEA. The combined plot of dispersive, specific (acid-base) and the total surface energy

of the samples are presented in Figure 2, Figure 3 and Figure 4. The profiles show that all samples are energetically heterogeneous, meaning the surface energy changes as a function of surface coverage. However the neat epoxy is energetically more heterogenous than the fibre samples, and the eopxy has a clearly higher specific (acid-base) and total surface energy.

From the two fibre samples the *"std wo a."* fibre possesses a slightly higher specific surface energy. The γ_S^{AB} of the *std* and *CR* fibres are only sligthly different but the actual ΔG_{SP} numbers differ clearly. The ΔG_{SP} profiles as a result of the interactions with the polar probe molecules are shown in Figure 5 and Figure 6. Higher ΔG_{SP} values can be attributed to a higher concentration of polar surface groups or different surface groups with higher specific surface energy. The ΔG_{SP} values of polar probes, especially the ones for Acetone and Acetonitrile, are higher on the *"std wo a."* sample. The significant difference on the specific free energy changes (ΔG_{sp}) between the samples are presented in more detail in Figure 7. The *"std wo a."* sample shows stronger interaction with most of the polar probes.

The surface chemistry of the samples was determined using the Gutmann acid (K_a) and base (K_b) numbers, determined based on the Gutmann approach. Values of the sample were calculated using the ΔG_{SP} values of polar probes at that particular surface coverage. Figure 8 shows that the K_b for the samples is consistently higher than K_a, indicating that the surface of the samples is more basic in nature. There is notable difference between the K_b values of the two cellulose fibre types. The neat epoxy has a higher K_a and K_b value due to its higher specific surface energy value.

Based on the reproducibility of the instrument, the standard deviation of the surface energy results in case of the fibres is about 0.15 – 0.29 mJ/m^2. Thus the measured relatively small difference (1mJ/m^2) at infinite dilution between the fibres is significant.

The measured dispersive surface energy of the Cordenka fibre is well in the range of the values obtained by Heng et al. [11] for other regenerated cellulose fibres (39.0 mJ/m^2) or

natural fibres as bamboo, sisal, flax or hemp (38.9-43.1 mJ/m²). For highly crystalline cellulose a dispersive surface energy of 60 to 66 mJ/m² was measured. Dorris and Grey reported a dispersive surface energy between 45 and 48 mJ/m² for cotton cellulose, measured with the same absobate and at a similar temperature. Also the K_a values are in good agreement with the literature. Here values between 0.08 and 0.12 are reported. The base number is rather high, between 0.00 and 0.41, compared to the values reported in literature. However the base number is known to vary significantly depending on differing amounts of cellulose in the fibre surface [11]. The surface tension of the cured epoxy can be compared to values measured by Ramathan et al. [8]. The specific surface energy is in the same range as the reported value of 16.5 ± 1.5 mN/m. The dispersive and total surface energy are higher as the measured values of 26.1 ± 1.3 and 42.6 ± 2.0 mN/m.

According to the measured iGC results of the specific surface energy and the K_a and K_b values the epoxy matrix is more polar than the cellulose fibres. From the two cellulose fibre samples the *"std wo a."* fibre possesses a slightly higher specific surface energy resulting from an increased interaction with polar probes. As the epoxy sample is highly polar the higher specific surface energy of the *"std wo a."* sample leads to an higher adhesion to the epoxy. The K_a value is about the same for both fibre samples, however *"std wo a."* has a higher base number (K_b), which again can lead to a stronger interaction with the epoxy and thus a higher interfacial adhesion compared to the "*CR* wo a." fibres. This can also be quantified in the pair specific interaction parameters (I_{sp}) which is calculated by the Equation (4) from the mean K_a and K_b values of the neat epoxy and the cellulose fibre samples. The I_{sp} for the neat epoxy - *"std wo a."* pair is 0.0932 and clearly higher than the I_{sp} of the neat epoxy – *"CR wo a."* pair of 0.0885.

The thermodynamic work of cohesion of the samples and the thermodynamic work of adhesion of the different composites were calculated with equation (6) and (7) and are shown in Figure 9. The dashed lines show that the work of adhesion between the neat epoxy and the

"std wo a." fibres is slightly higher than that of the *"CR wo a."* fibres and the neat epoxy suggesting that the bond of the *standard* fibre to the matrix is stronger than of the *CR* fibres.

4.3 Fibre pull-out length

The iGC exposed differences in surface chemistry between the *std* and *CR* fibre suggesting a stronger adhesion of the *"std wo a."* fibre to the epoxy. To further quantify the differences in interfacial shear strength of the two fibre types with and without avivage the fibre pull-out-lengths were measured. The results are shown in Figure 10. Within the same fibre type the samples without avivage show longer pull-out lengths which suggests a weaker interfacial shear strength, confirming that the avivage improves the adhesion of the Cordenka fibre to the matrix. This difference is significant for the *std* fibre (pairwise Wilcoxon rank sum test, $\alpha = 5$ %, $p = 0.03$) but not for the *CR* fibre (pairwise Wilcoxon rank sum test, $\alpha = 5$ %, $p = 0.38$). The pull-out length of the *CR* fibres is significantly higher than the one of the *standard* Cordenka fibres (pairwise Wilcoxon rank sum test, $\alpha = 5$ %, $p < 0.01$). As can be seen in Figure 10 the median pull-out length of the *CR* fibres is one order of magnitude larger than that of the *std* fibres. A higher tensile strength leads to higher pull-out lengths as with the same interfacial shear strength more area is needed to transfer enough stress from the matrix to the fibre to cause its breakage. Thus higher fibre pull-out lengths would occur with the *CR* fibre even if the interfacial shear strength was the same for both fibre types. To take in to account the higher tensile strength of the *CR* fibre the corrected pull-out lengths are calculated as explained above and listed in Table 2. Even with this correction the difference between the two fibre types *CR* and *std* is significant and only slightly smaller. This proves that a clear difference in interfacial shear strength can be measured that is not caused by the differences in the tensile strength of the fibres.

The higher pull-out lengths are a measure for the weaker fibre-matrix adhesion of the *CR* fibre to the matrix compared to the *standard* Cordenka fibre. These results correspond to the measured surface energies. The higher pair specific interaction parameter I_{sp} and the higher thermodynamic work of adhesion of the neat epoxy - *"std wo a."* pair result in significantly higher interfacial shear strength. This relation has been measured before for carbon fibres in an epoxy matrix by Schultz et al. [15] for the I_{sp} and by Ramanathan et al. [8] for the thermodynamic work of adhesion. Park et al. [29] observed a directly proportional dependency of the interfacial shear strength and both the work of adhesion and the polar surface energy.

As mentioned before the interfacial adhesion plays a crucial role in the mechanical properties of a composite. For the impact strength three main mechanisms for energy absorption have been identified: debonding, fracture and fibre pull-out. Thomason & Vlug stated that this means that an improved fibre-matrix adhesion will result in a shorter debond length and subsequently pull-out length. Which results in a lower energy absorptions and a decrease in impact strength. Thomason & Vlug suppose that the improvement of the fibre-matrix adhesion in order to increase the tensile strength has to be combined with an increase in fibre strength if the impact strength are not supposed to decrease. On the other hand he calculated an increase in debond length, and subsequently pull-out length and energy absorption, if the fibre-matrix adhesion decreases and the fibre tensile strength remains constant [9]. As the *standard* Cordenka fibre shows a lower tensile strength and a higher pair specific interaction parameter I_{sp} with the epoxy matrix, the lower pull-out lengths and impact strengths are reasonable. Erdmann & Ganster investigated the influence of fibre-matrix adhesion of ductile man-made cellulose fibres in a comparably brittle PLA matrix [30]. They found that an increase in fibre-martix adhesion by means of an adhesion promoter resulted in a moderate increase in tensile strength and had no influence on the notched Charpy impact strength of the injection moulded samples. A weakening of the interfacial bonding leads to a decrease in the

tensile strength but to an increase of the Charpy impact strength by 400 %. SEM images of the fracture surface showed a clear increase in fibre pull-out with decreasing fibre-matrix adhesion and increasing notched Charpy impact strength.

The measured pull-out lengths of all four Cordenka fibre types show the same trend. The higher the earlier measured Charpy impact strengths of the four different samples, the higher the pull-out length. In Figure 11 the Charpy impact strength is plotted as a function of fibre pull-out length. A nearly linear relationship can be observed. This seems reasonable as in long fibre reinforced composites fibre debonding and pull-out is supposed to be the most important energy dissipation mechanism. The fibre pull-out length is directly proportional to the contact area between the fibre and matrix at which frictional forces occur during fibre pull-out.

These results also support the hypothesis that the interfacial shear strength between the *CR* fibre and the epoxy is weaker than with the *std* fibres resulting in a stronger crack deflection and more energy absorption due to friction during fibre pull-out process.

5 Conclusion

The results of the conducted experiments show clearly that the adhesion of the Cordenka *CR* fibres to the epoxy matrix is weaker than that of the *standard* Cordenka fibres. The iGC measurements revealed that the *CR* Cordenka fibres possess a lower specific surface energy and are less polar in nature resulting in a lower pair specific interaction parameter and lower work of adhesion with the epoxy, compared to the *standard* fibre. The lower adhesion of the *CR* fibres is proven also by the measured higher fibre-pull-out lengths. These cause a stronger crack deflection as well as energy dissipation and correspond well with the previously measured higher Charpy impact strengths.

The in this study obtained results support the hypothesis that the measured differences in Charpy impact strength are caused by the differing surface properties (dispersive surface

energy and pair specific interaction parameter) of the *CR* and the *standard* fibre, which results in different interfacial shear strengths.

Acknowledgements

Finally, many thanks to the referees for their valuable comments. Parts of this research have been supported by a grant from the Cordenka GmbH & Co. KG, Obernburg, DE. We gratefully acknowledge the financial support of the Cordenka Student Scholarship. The authors would like to thank especially Annika Fritsch and Felix Weiler for their help and efforts in determining the fibre pull-out lengths.

6 Literature

References

[1] Klemm D, Heublein B, Fink H, Bohn A. Cellulose: faszinierendes Biopolymer und nachhaltiger Rohstoff. Angew. Chem. 2005;117(22):3422–58.

[2] Ganster J, Fink H. Novel cellulose fibre reinforced thermoplastic materials. Cellulose 2006;13(3):271-280.

[3] Graupner N. Improvement of the Mechanical Properties of Biodegradable Hemp Fiber Reinforced Poly(lactic acid) (PLA) Composites by the Admixture of Man-made Cellulose Fibers. Journal of Composite Materials 2009;43(6):689–702.

[4] Mader A, Volkmann E, Einsiedel R, Müssig J. Impact and Flexural Properties of Unidirectional Man-Made Cellulose Reinforced Thermoset Composites. J Biobased Mat Bioenergy 2012;6(4):481–92.

[5] Pizzi A, Mittal KL. Handbook of adhesive technology. 2nd ed. New York: M. Dekker; 2003.

[6] Riedl B, Matuana LM. Inverse gas chromatography of fibers and polymers. Encyclopedia of Surface and Colloid Science 2006:2842–55.

[7] Ramanathan T, Bismarck A, Schulz E, Subramanian K. Investigation of the influence of surface-activated carbon fibres on debonding energy and frictional stress in polymer-matrix composites by the micro-indentation technique. Composites Science and Technology 2001;61(16):2511–8.

[8] Tze, William T. Y., Gardner DJ, Tripp CP, O'Neill SC. Cellulose fiber/polymer adhesion: effects of fiber/matrix interfacial chemistry on the micromechanics of the interphase. Journal of Adhesion Science and Technology 2006;20(15):1649–68.

[9] Thomason JL, Vlug MA. Influence of fibre length and concentration on the properties of glass fibre-reinforced polypropylene: 4. Impact properties. Composites Part A: Applied Science and Manufacturing 1997;28(3):277–88.

[10] Kim J, Mai Y. High strength, high fracture toughness fibre composites with interface control—A review. Composites Science and Technology 1991;41(4):333–78.

[11] Heng, Jerry Y. Y., Pearse DF, Thielmann F, Lampke T, Bismarck A. Methods to determine surface energies of natural fibres: a review. Composite Interfaces 2007;14(7-9):581–604.

[12] Belgacem MN, Gandini A. The surface modification of cellulose fibres for use as reinforcing elements in composite materials. Composite Interfaces 2005;12(1-2):41–75.

[13] Abdelmouleh M, Boufi S, Belgacem MN, Dufresne A, Gandini A. Modification of cellulose fibers with functionalized silanes: Effect of the fiber treatment on the mechanical performances of cellulose-thermoset composites. J. Appl. Polym. Sci. 2005;98(3):974–84.

[14] Bledzki A. Composites reinforced with cellulose based fibres. Progress in Polymer Science 1999;24(2):221–74.

[15] Schultz J, Lavielle L, Martin C. The Role of the Interface in Carbon Fibre-Epoxy Composites. The Journal of Adhesion 1987;23(1):45–60.

[16] Clint JH. Adhesion and components of solid surface energies. Current Opinion in Colloid & Interface Science 2001;6(1):28–33.

[17] Mukhopadhyay P, Schreiber HP. Aspects of acid-base interactions and use of inverse gas chromatography. Colloids and Surfaces A: Physicochemical and Engineering Aspects 1995;100:47–71.

[18] van Asten A, van Veenendaal N, Koster S. Surface characterization of industrial fibers with inverse gas chromatography. Journal of Chromatography A 2000;888(1–2):175–96.

[19] Thielmann F, Levoguer C. Application Note 303. Alperton London, United Kingdom: Surface Measurement Systems UK Ltd; 2005.

[20] Cordeiro N, Silva J, Gomes C, Rocha F. Bentonite from Porto Santo Island, Madeira archipelago: surface properties studied by inverse gas chromatography. Clay Miner. 2010;45(1):77–86.

[21] Riddle FL, Fowkes FM. Spectral shifts in acid-base chemistry. 1. van der Waals contributions to acceptor numbers. J. Am. Chem. Soc. 1990;112(9):3259–64.

[22] Papirer E, Brendle E, Ozil F, Balard H. Comparison of the surface properties of graphite, carbon black and fullerene samples, measured by inverse gas chromatography. Carbon 1999;37(8):1265–74.

[23] Voelkel A, Krysztafkiewicz A. Acid-based properties of silicas modified by organic compounds as determined by inverse gas chromatography. Powder Technology 1998;95(2):103–8.

[24] Van Oss, Carel J., Chaudhury MK, Good RJ. Interfacial Lifshitz-van der Waals and polar interactions in macroscopic systems. Chem. Rev. 1988;88(6):927–41.

[25] Abbott JR, Higgins BG. Surface tension of a curing epoxy. J. Polym. Sci. A Polym. Chem. 1988;26(7):1985–8.

[26] Wu S. Polymer interface and adhesion. New York: M. Dekker; 1982.

[27] Kelly A, Tyson WR. Tensile properties of fibre-reinforced metals: Copper/tungsten and copper/molybdenum. Journal of the Mechanics and Physics of Solids 1965;13(6):329–50.

[28] Graupner N, Albrecht K, Hegemann D, Müssig J. Plasma modification of man-made cellulose fibers (Lyocell) for improved fiber/matrix adhesion in poly(lactic acid) composites. J. Appl. Polym. Sci. 2013;128(6):4378–86.

[29] Park J, Kim D, Kim S. Erratum to: "Improvement of interfacial adhesion and nondestructive damage evaluation for plasma-treated PBO and Kevlar fibers/epoxy composites using micromechanical techniques and surface wettability". Journal of Colloid and Interface Science 2003;268(1):271.

[30] Erdmann J, Ganster J. Tailor-made PLA and PHB based cellulose fibre composites through coupling or anti-coupling agents. In 8th International Symposium "Materials made of Renewable Resources" 2010;Erfurt, Germany.

Table 1: The BET specific surface area determined from octane sorption isotherm

Sample	Sorption Constant	Monolayer Capacity in mMol/g	BET Specific Surface Area in m^2/g	R^2
"*Std wo a.*" sample	2.6561	0.0007	0.2543	0.9998
"*CR wo a.*" sample	2.5859	0.0007	0.2577	0.9995
Neat epoxy sample	1.6809	0.0003	0.1018	0.9868

Table 2: Fibre pull-out length, fibre tensile strength and Charpy impact strength of the differend Cordenka samples. ***(Pull-out length values: median ± mad; tensile strength & impact strength taken from Mader et al. [5]: mean ± st.dev.)***

Sample	Pull-out length in µm	Corrected pull-out length in µm	Tensile strength in MPa	Impact strength in kJ/m²
"Std w a."	18 ± 26	18 ± 26	652.2 ± 21.2	140.0 ± 8.8

"Std wo a."	39 ± 29	38 ± 29	662.0 ± 25.6	188.2 ± 9.9
"CR w a."	113 ± 92	97 ± 79	759.4 ± 62.5	298.5 ± 22.3
"CR wo a."	120 ± 78	92 ± 60	850.0± 77.0	316.4 ± 15.8

1

2

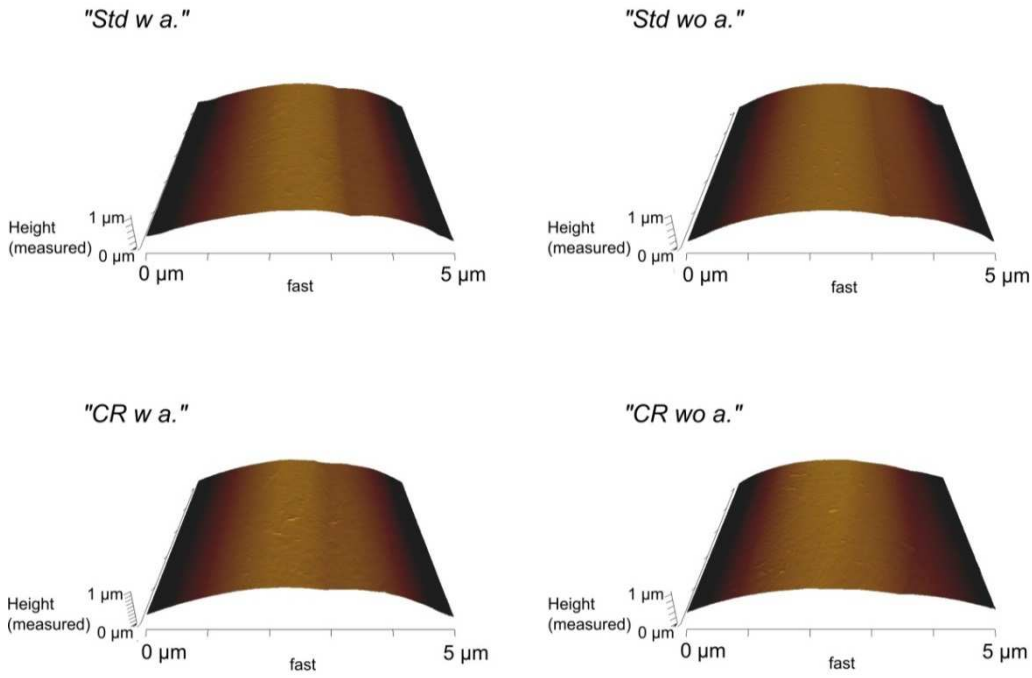

Figure 1: AFM surface profiles of the different Cordenka samples. On the micro scale there is no difference in the surface morphology recognizable.

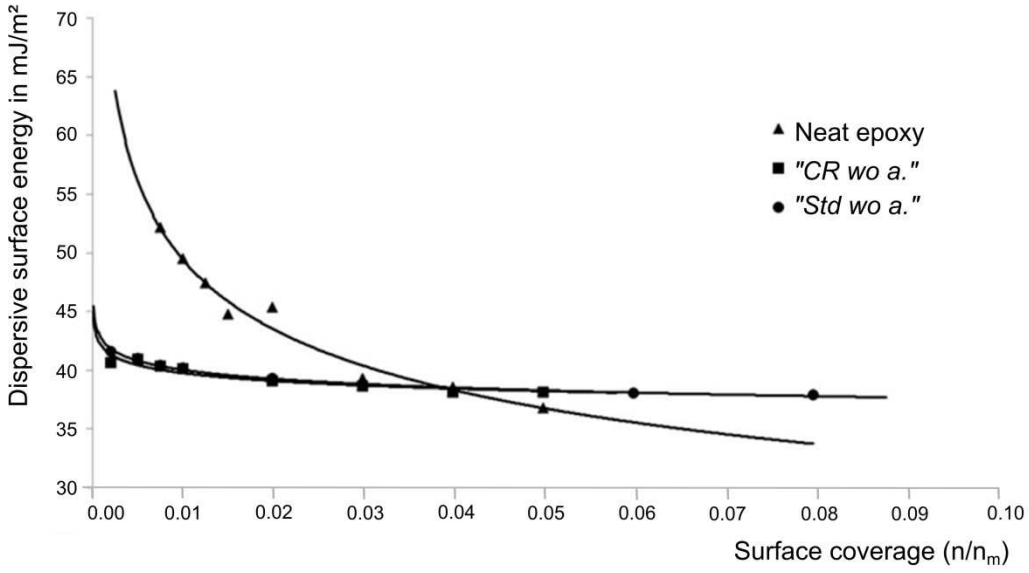

Figure 2: Comparison of the dispersive surface energy profile (as function of surface coverage) of the samples. The surface coverage is a dimensionless quantity. It is the ratio of moles (n/n_m), n_m is the number of moles for the mono layer coverage, and n is the injected/adsorbed moles of molecules.

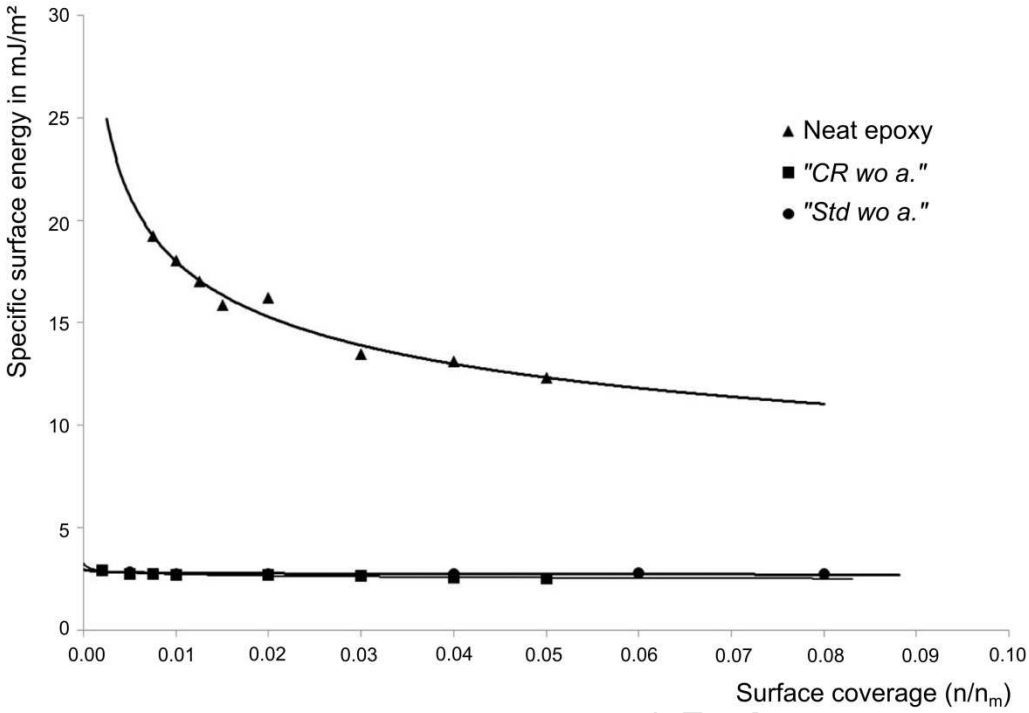

Figure 3: Comparison of the specific surface energy profile (as function of surface coverage) of the samples.

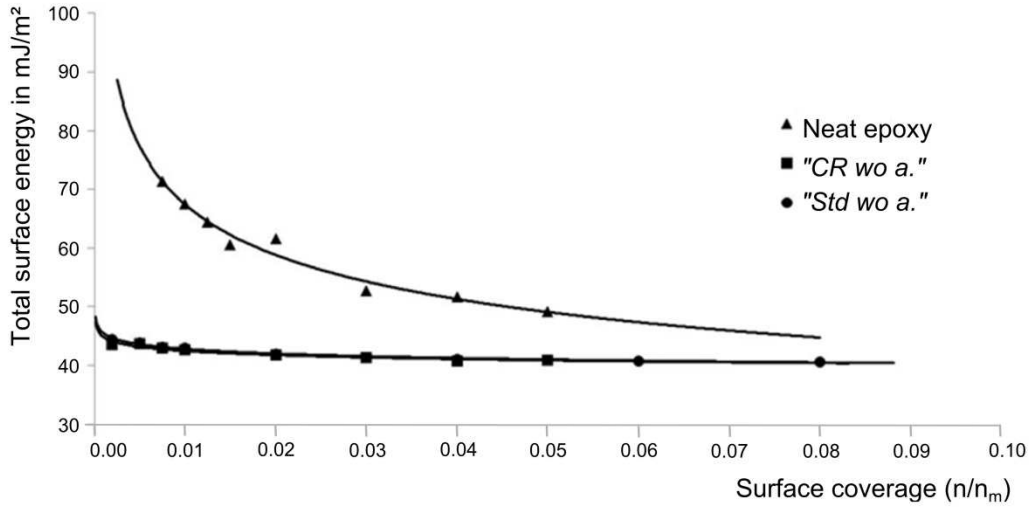

Figure 4: Comparison of the total surface energy profile (as function of surface coverage) of the samples.

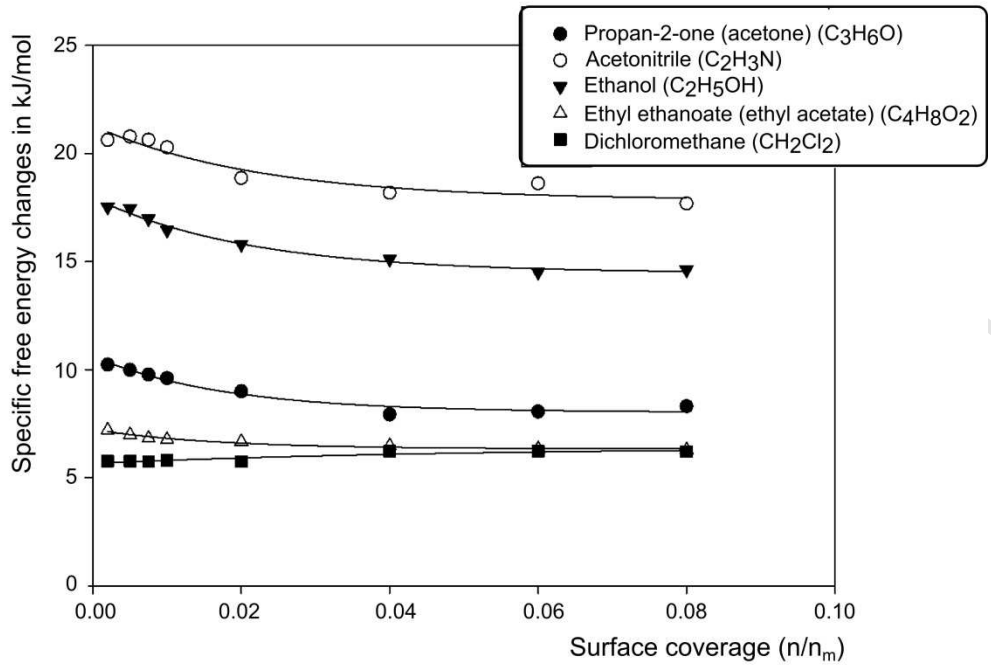

Figure 5: Specific (acid-base) free energy profiles of different solvents for the *"std wo a."* sample.

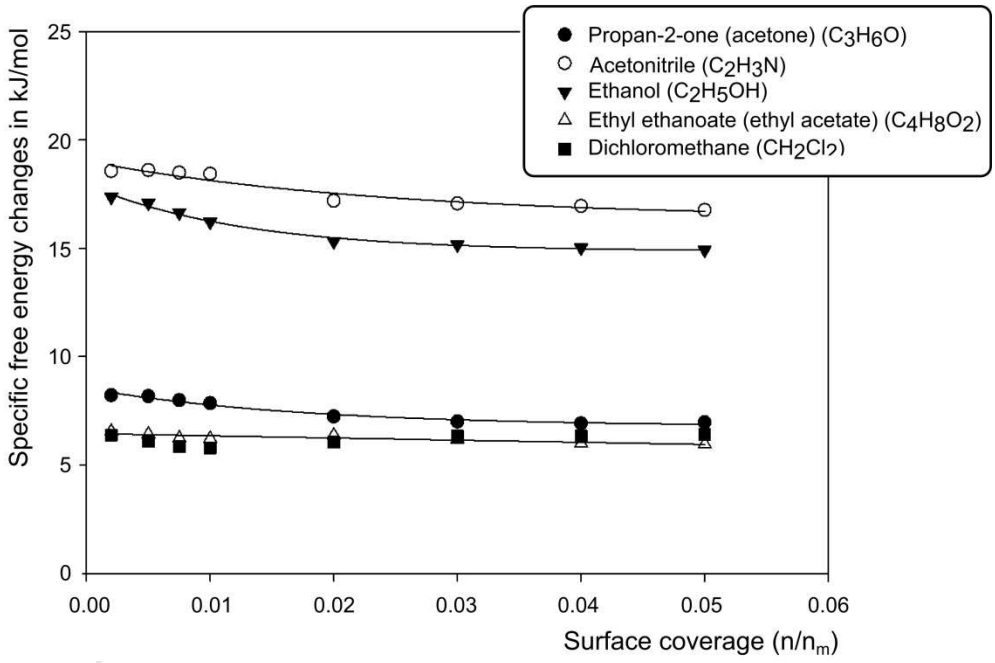

Figure 6: Specific (acid-base) free energy profiles of different solvents for the *"CR wo a."* sample.

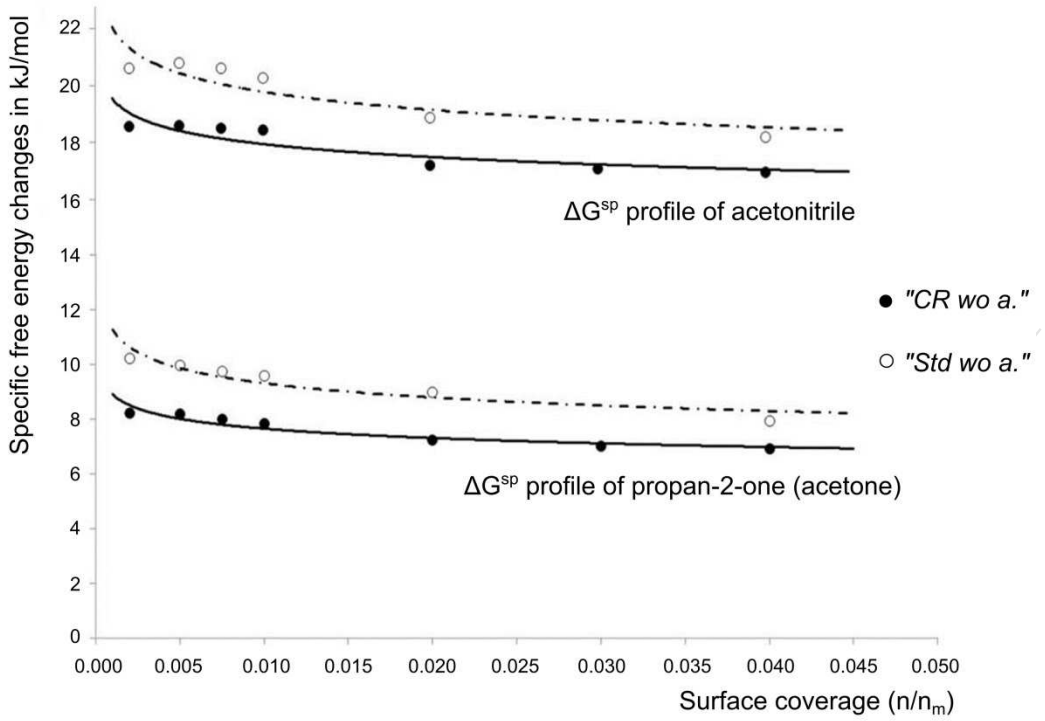

Figure 7: Specific free energy changes of the acetonitrile (C_2H_3N) and propan-2-one (acetone) (C_3H_6O) on *"CR wo a."* and *"std wo a."* samples. $\triangle G^{sp}$ profile of acetonitrile and propan-2-one (acetone).

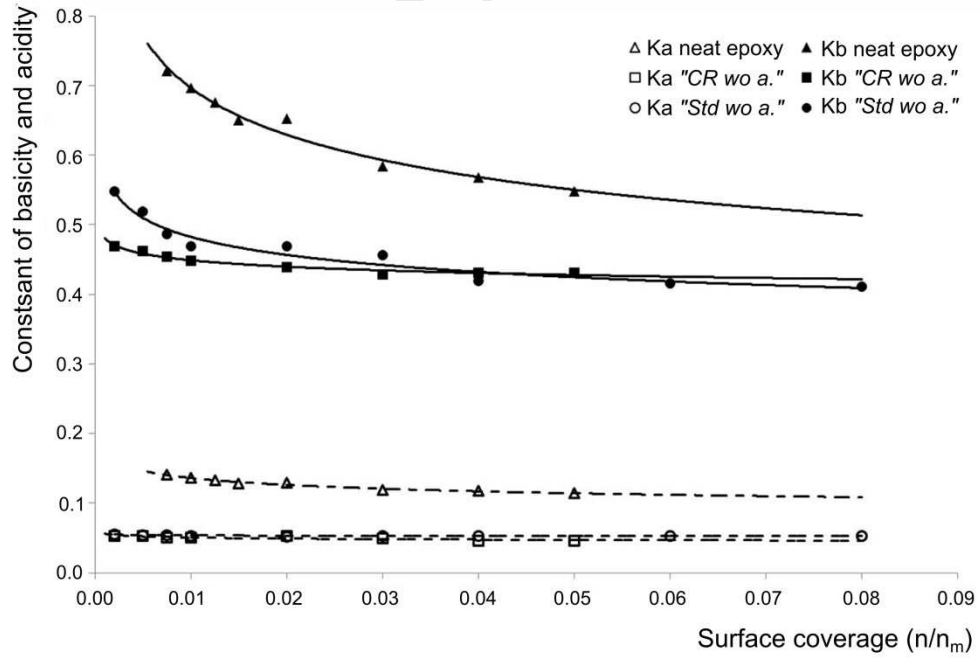

Figure 8: Gutmann acid (K_a) and base (K_b) numbers profiles of the samples.

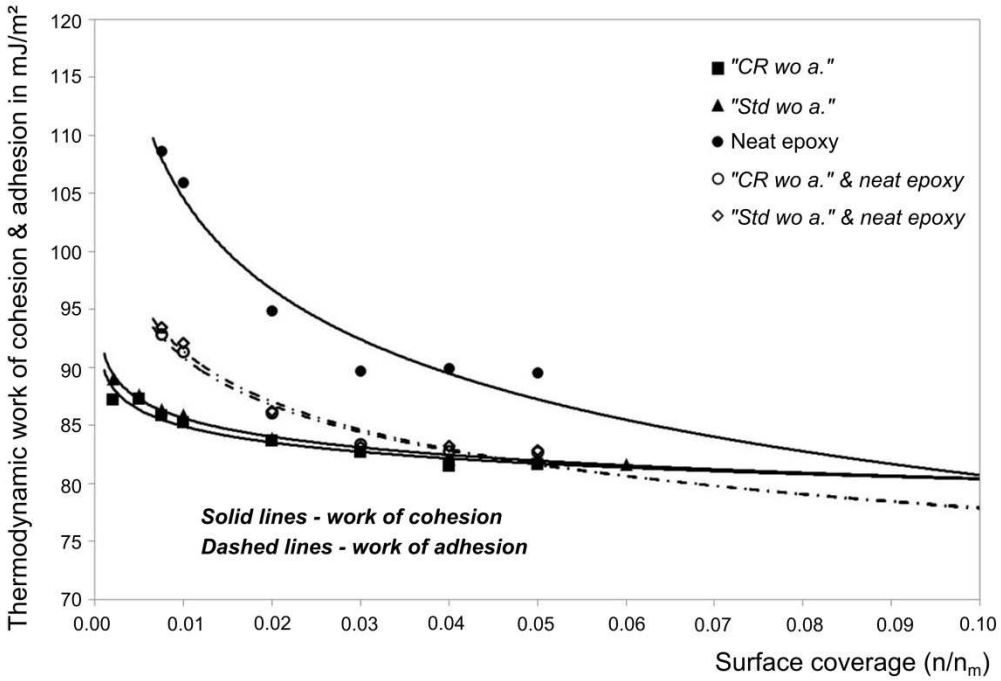

Figure 9: The thermodynamic work of cohesion of the samples and work of adhesion of the sample pairs.

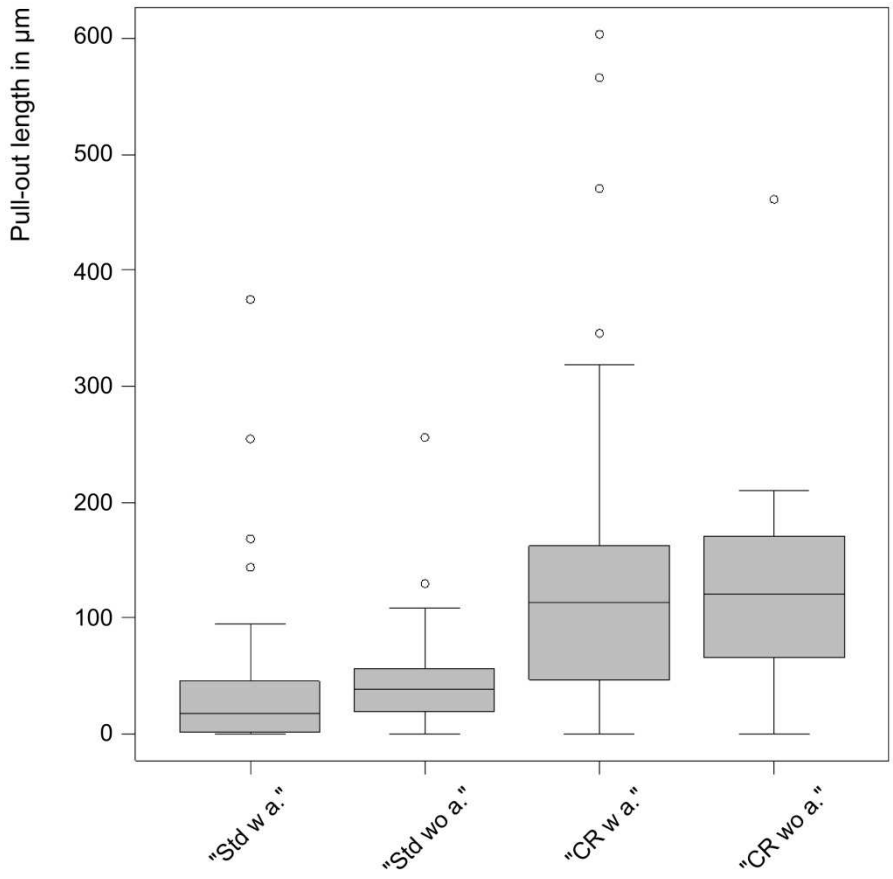

Figure 10: Fibre pull-out length of different Cordenka samples.

1

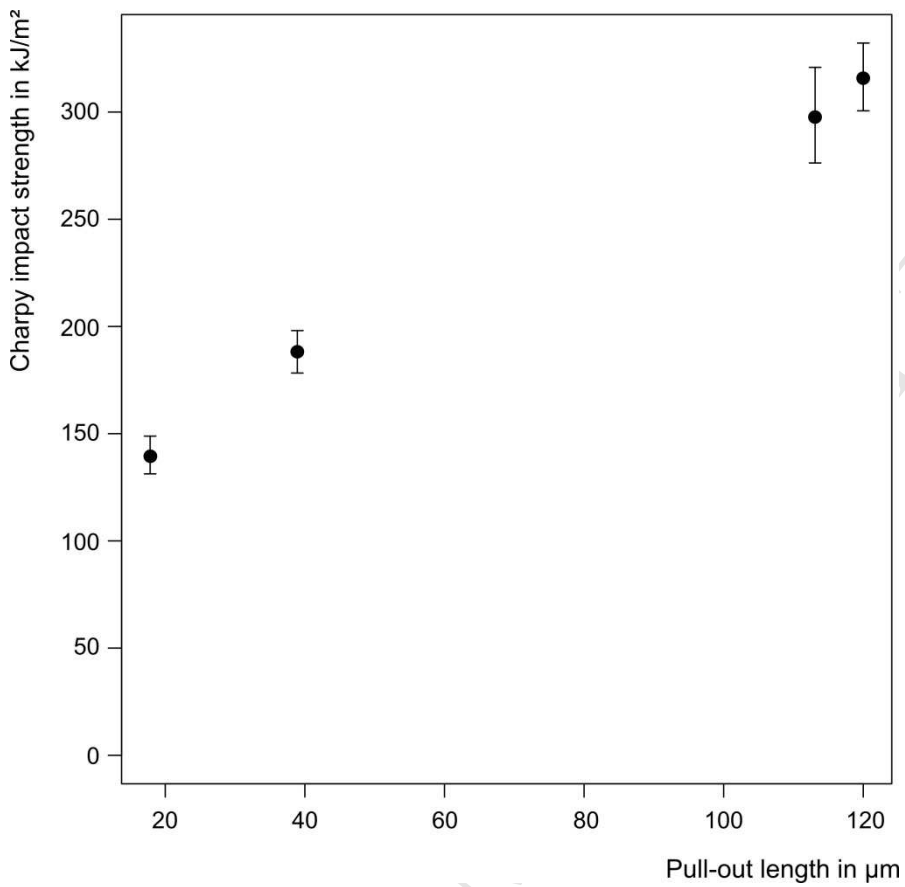

2

3 **Figure 11: Charpy impact strength versus measured fibre pull-out length.**

4

5